Hexadecapole deformation effects in subbarrier fusion reactions

J. O. Fernández Niello,* M. di Tada, A. O. Macchiavelli,† A. J. Pacheco, D. Abriola, M. Elgue, A. Etchegoyen, M. C. Etchegoyen, S. Gil, and J. E. Testoni

TANDAR, Departamento de Física, Comisión Nacional de Energía Atómica, Avenida del Libertador 8250, 1429 Buenos Aires, Argentina

(Received 25 September 1990)

Possible effects of hexadecapole nuclear deformations on subbarrier fusion cross sections are investigated. The ^{16}O on ^{166}Er and ^{176}Yb reactions have been measured at beam energies ranging from 64 to 100 MeV. The ^{166}Er and ^{176}Yb data and already existing ^{154}Sm data were analyzed in terms of a model including both quadrupole and hexadecapole deformations. Theoretical predictions follow qualitatively the trend of the experimental data.

I. INTRODUCTION

The study of fusion reactions at bombarding energies below the Coulomb barrier has been the subject of much theoretical and experimental effort in the last years. While different effects such as zero-point oscillations of the nuclear shape, nucleon transfer, and neck formation have been considered in order to explain observed enhancements of fusion cross sections $\sigma_{\rm fus}$, the role of the nuclear static quadrupole deformation β_2 has been well established in fusion measurements of ^{16}O on various even Sm isotopes.[1] For a fixed bombarding energy, the effect of such a deformation is to bring the nuclear surfaces closer together at orientation angles in the vicinity of the poles, which results in an increase of the fusion rates when averaged over all orientation angles.

The possible role of positive and negative hexadecapole deformations β_4 in the enhancement of fusion cross sections below the barrier has been recently investigated using a coupled-channel formalism which incorporates shape effects within the sudden-approximation scheme.[2] The model predicts that the inclusion of hexadecapole deformations may give rise to substantial deviations in the subbarrier fusion excitation functions with respect to a pure quadrupole shape. It predicts that positive hexadecapole deformations will always increase fusion cross sections relative to a pure prolate shape. On the other hand, the model suggests that negative hexadecapole deformations seem to have a twofold effect: They may reduce cross-section enhancements for smaller values, whereas they would increase them for larger values. A more quantitative assessment of this effect for the smaller range of β_4 values can be obtained from Fig. 1. The enhancement factor ϵ in the figure is defined as

$$\epsilon = \frac{\sigma_{\rm fus}(E_{\rm c.m.} < V_B)_{\beta_2,\beta_4 \neq 0}}{\sigma_{\rm fus}(E_{\rm c.m.} < V_B)_{\beta_2,\beta_4 = 0}} , \quad (1)$$

and it is plotted as a function of β_4 for a constant value $\beta_2 = 0.23$ at $E_{\rm c.m.} = 60$ MeV, where $E_{\rm c.m.}$ is the center-of-mass energy and V_B is the interaction-barrier height. Nuclear profiles with negative, zero, and positive values of β_4 are shown at the bottom of the figure. The dotted curves indicate prolate deformation only. The behavior exhibited by the enhancement function may be understood in terms of both effective barrier heights and statistical weights as a function of the angle between the symmetry axis of the deformed target and the line joining the centers of the two nuclei (see Ref. 2).

The influence of large negative hexadecapole deformations has been invoked in theoretical calculations[3] for the ^{16}O + ^{184}W fusion reaction at subbarrier energies in order to help to quantify the above-described enhancement. Not much work has been performed from an experimental standpoint. In this respect, fusion of ^{16}O projectiles with ^{232}Th targets[4] has been measured and analyzed including the sizable positive hexadecapole deformations of ^{232}Th. On the other hand, enhancement of subbarrier fusion cross sections due to negative hexadecapole defor-

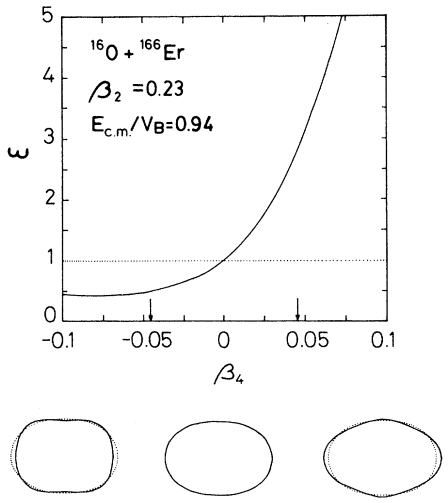

FIG. 1. Enhancement factor ϵ as a function of the hexadecapole deformation β_4. Also shown are the nuclear profiles with negative, zero, and positive values of β_4. The arrows indicate the approximate β_4 values for ^{176}Yb (negative) and ^{154}Sm (positive).

mations has been measured for ^{16}O + Hf and W.[5]

In the present work, we report on an attempt to isolate the effect of negative and positive hexadecapole deformations by choosing target nuclei with approximately the same value of the static quadrupole deformation parameter β_2. For this purpose, the systems $^{16}O+^{154}Sm$, ^{166}Er, and ^{176}Yb have been chosen. The use of a doubly magic nucleus as projectile is convenient since it singles out shape effects that are to be attributed only to the targets. From α-scattering experiments,[6] these three targets have been determined to have approximately the same $\beta_2=0.23$, whereas the static hexadecapole parameter β_4 ranges from -0.045 for ^{176}Yb to 0.045 for ^{154}Sm. The ^{166}Er nucleus, characterized by $\beta_4\approx 0$, will be used as a reference for a pure quadrupole shape.

II. EXPERIMENT

The measurements were carried out at the 20-MV tandem accelerator of the TANDAR Laboratory in Buenos Aires. Enriched targets of ^{166}Er (96.24%) and ^{176}Yb (96.68%) with thickness of 67 and 72 $\mu g/cm^2$, respectively, were bombarded with ^{16}O projectiles with energies between 64.5 and 103 MeV. The systematic uncertainty on the beam energy was 0.4%.[7]

The data for $^{16}O+^{154}Sm$ have been taken from Ref. 1, except for the point at 64.5 MeV, which was measured as an additional check of the experimental procedure. For the other two systems ($^{16}O+^{166}Er$,^{176}Yb) evaporation-residue cross sections as a function of bombarding energy have been determined by measuring the activity of the delayed x rays emitted in the subsequent decay. The evaporation residues were collected on aluminum catcher foils placed immediately behind the targets. After irradiations lasting typically 2 h, these catchers were removed from the scattering chamber and placed in front of an x-ray counter in order to perform the off-line analysis. For the ^{176}Yb target at the bombarding energies at which the $4n$-evaporation channel was strong, the irradiation time was set to 12 h due to the long half-life of the ^{188}Pt evaporation residue.

The energy resolution of the x-ray detector was 700 eV (full width at half maximum) at 60 keV, and its absolute efficiency was 16% in the energy range of 40–60 keV. Further details of the experimental setup and data analysis may be found in Refs. 8 and 9.

An off-line energy spectrum of $^{16}O+^{176}Yb$ for a bombarding energy of 90 MeV is shown in Fig. 2. This figure shows the different x-ray peaks from atoms with different atomic numbers. These atoms are produced through the radioactive decays of the various evaporation residues within a chosen time interval.

Assuming negligible contributions from fission decay, fusion cross sections were obtained as the sum of the yields of individual light-particle evaporation channels which are readily obtained via a χ^2 minimization routine. For this purpose, the time dependence of the $K\alpha$ x-ray yields for both parent and daughter activities are calculated from the known half-lives and absolute number of $K\alpha$ x rays produced per decay of each isotope in each mass chain.[10] Then the cross sections for the different

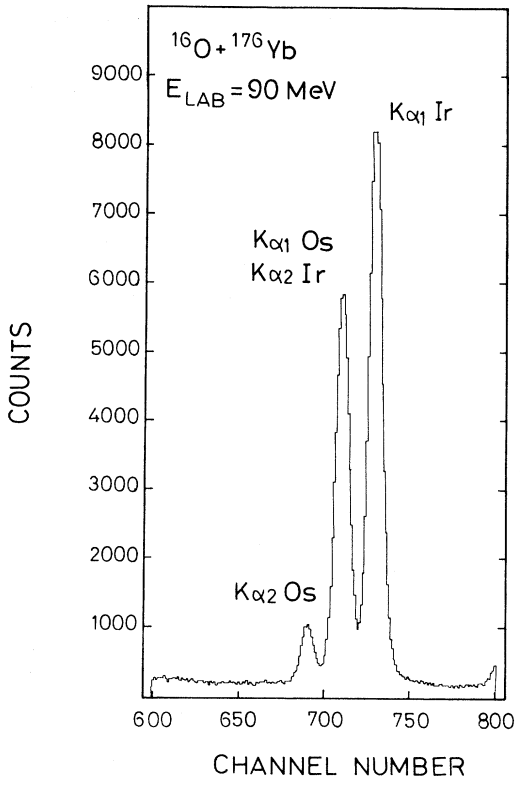

FIG. 2. Off-line energy spectrum from $^{16}O+^{176}Yb$ for a bombarding energy of 90 MeV showing the delayed x rays emitted in the subsequent decays from the evaporation residues.

evaporation residues were deduced by minimizing the χ^2 function constructed from the experimental number of detected x rays and the theoretical calculations.

Figure 3 shows the off-line time dependence of the activities for $^{16}O+^{166}Er$ for an impinging energy of 75

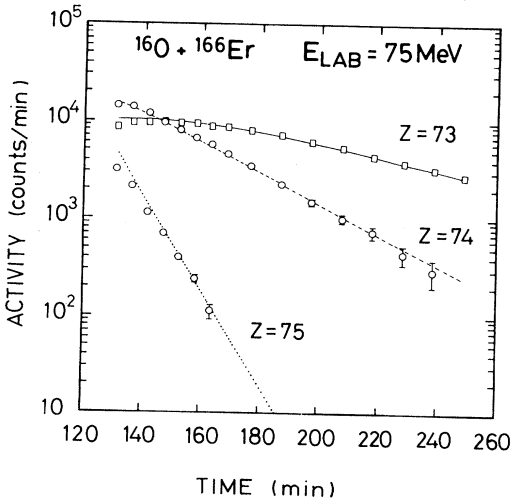

FIG. 3. Off-line time dependence of the activities of decays from evaporation residues produced by the $^{16}O+^{166}Er$ reaction at $E_{lab}=75$ MeV. Calculated fits for the different elements are also shown.

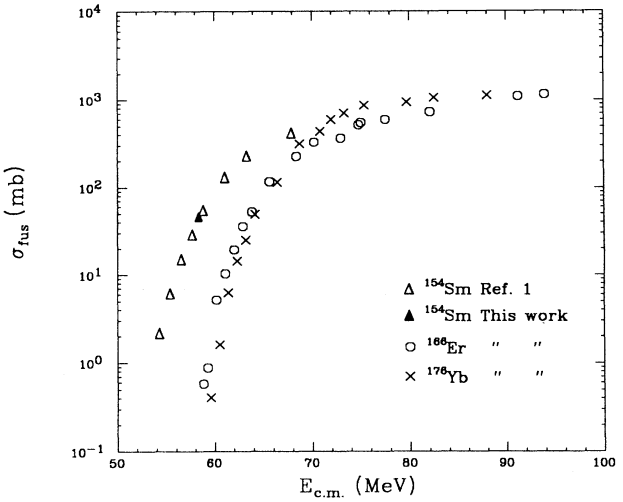

FIG. 4. Fusion cross sections versus center-of-mass energies.

MeV. The calculated best fits for the different elements are represented by the curves.

III. RESULTS AND DISCUSSION

Fusion cross sections as a function of center-of-mass energies are displayed in Fig. 4. The data points show the common behavior for near-barrier reactions, namely, an almost exponential fall at subbarrier energies, while for the highest energies the cross sections follow the geometrical pattern

$$\sigma_{\text{fus}} = \pi R_B^2 \left[1 - \frac{V_B}{E_{\text{c.m.}}} \right] . \tag{2}$$

The interaction-barrier height V_B and its radial position R_B were obtained from a least-squares fit to the corresponding experimental points at energies above the barrier. The fitted values for r_B—defined as $R_B = r_B(A_p^{1/3} + A_t^{1/3})$— and V_B obtained for the three systems are summarized in Table I.

In order to compare the three systems, the data points are recast in a different manner. First, we define the *reduced cross sections* σ_{red} as

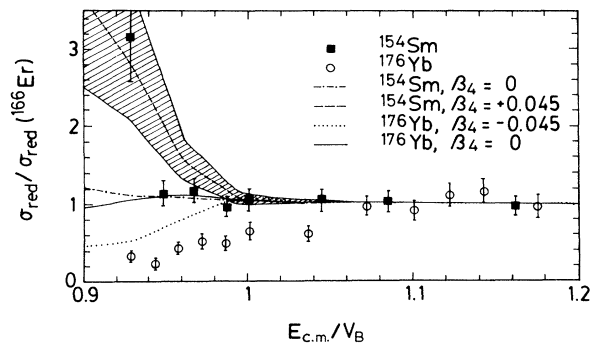

FIG. 5. Reduced fusion cross sections for ^{154}Sm and ^{176}Yb targets normalized to that for the ^{166}Er target and plotted as a function of $E_{\text{c.m.}}/V_B$ (see text for more details). The ^{154}Sm data are taken from Ref. 1.

TABLE I. Calculated values of interaction-barrier heights V_B and their radius parameters r_B for the different targets.

Target	V_B (MeV)	r_B (fm)
^{154}Sm	58.55	1.254
^{166}Er	63.79	1.334
^{176}Yb	64.12	1.548

$$\sigma_{\text{red}} = \frac{\sigma_{\text{fus}}}{\pi R_B^2} , \tag{3}$$

in order to remove any difference trivially related to geometric aspects of the reaction. Then the reduced cross sections for both ^{154}Sm and ^{176}Yb targets are normalized to the value for the ^{166}Er target and plotted as a function of $E_{\text{c.m.}}/V_B$. In this way any structure-related effects will become more noticeable at subbarrier energies. Because of the fact that the different reactions have not been measured at exactly the same $E_{\text{c.m.}}/V_B$ values, the ^{166}Er normalization has been made using an exponential interpolation of the ^{166}Er experimental data points. The results thus obtained are displayed in Fig. 5. The full curves are calculations performed with the code CCDEF,[1] including quadrupole and hexadecapole deformations given by the parameters of Ref. 6. Neither couplings to inelastic nor to transfer channels have been considered in the calculation. The hatched area around the curve corresponding to ^{154}Sm illustrates the sensitivity of the calculation with respect to uncertainties of $\pm 10\%$ in the values of β_2. Dashed curves correspond to the same cases considering *only* quadrupole shapes. The theory shows a large enhancement for ^{154}Sm and a smaller hindrance for ^{176}Yb.

The comparison between theory and experiment shows that the ^{154}Sm points are not at variance with the curve for positive β_4, although no definite conclusion can be drawn. The theory also predicts a decrease in the ^{176}Yb fusion cross sections for $\beta_4 = -0.045$, in agreement with the experiment, which helps to bridge the gap between theory and experiment. However, the measured cross sections are smaller than those indicated by either curve.

IV. CONCLUSIONS

The predicted influence exerted by hexadecapole deformations on subbarrier fusion reactions was investigated through the study of the reactions induced by ^{16}O projectiles on ^{176}Yb, ^{154}Sm, and ^{166}Er targets. These nuclei span a range from negative to positive values of β_4, while having approximately the same quadrupole deformation. The comparison between the excitation functions for ^{154}Sm ($\beta_4 > 0$) and ^{176}Yb ($\beta_4 < 0$) suggests that hexadecapole deformations may be playing a role as expected from theoretical estimates. It is apparent from Fig. 5 that these estimates do not suffice to quantitatively account for the experimental data for $\beta_4 < 0$.

This work was supported in part by the Consejo Nacional de Investigaciones Científicas y Técnicas, CONICET, Argentina.

*On leave at Sektion Physik, Universität München, 8046 Garching, Germany.
†On leave at Lawrence Berkeley Laboratory, U.C., Berkeley, CA 94720.

[1]R. G. Stokstad, Y. Eisen, S. Kaplanis, D. Pelte, U. Smilansky, and I. Tserruya, Phys. Rev. C **21**, 2427 (1980).
[2]J. O. Fernández Niello and C. H. Dasso, Phys. Rev. C **39**, 2069 (1989).
[3]M. J. Rhoades-Brown and V. E. Oberacker, Phys. Rev. Lett. **50**, 1435 (1983).
[4]H. Esbensen and S. Landowne, Nucl. Phys. **A467**, 136 (1987).
[5]J. R. Leigh, J. J. M. Bokhorst, D. J. Hinde, and J. O. Newton, J. Phys. G **14**, L55 (1988).
[6]D. L. Hendrie, N. K. Glendenning, B. G. Harvey, O. N. Jarvis, H. H. Duhm, J. Saudinos, and J. Mahoney, Phys. Lett. **26B**, 127 (1968).
[7]A. M. J. Ferrero, A. García, S. Gil, A. Etchegoyen, M. di Tada, A. J. Pacheco, D. Abriola, D. E. DiGregorio, M. Elgue, M. C. Etchegoyen, J. O. Fernández Niello, A. O. Macchiavelli, and J. E. Testoni, Nucl. Instrum. Methods B **42**, 389 (1989).
[8]D. E. DiGregorio, M. di Tada, D. Abriola, M. Elgue, A. Etchegoyen, M. C. Etchegoyen, J. O. Fernández Niello, A. M. J. Ferrero, S. Gil, A. O. Macchiavelli, A. J. Pacheco, J. E. Testoni, P. Silveira Gomes, V. R. Vanin, R. Liguori Neto, E. Crema, and R. G. Stokstad, Phys. Rev. C **39**, 516 (1989).
[9]A. J. Pacheco, J. O. Fernández Niello, and M. Elgue, Comput. Phys. Commun. **52**, 93 (1988).
[10]U. Reus and W. Westmeier, At. Data Nucl. Data Tables **29**, 1 (1983).